www.shd.org.rs

Journal of the Serbian Chemical Society

JSCS@tmf.bg.ac.yu • www.shd.org.rs/JSCS

J. Serb. Chem. Soc. *73* (12) 1197–1209 (2008)
JSCS–3799

UDC 546.78–261+546.92:544.6.004.2
Original scientific paper

Electrochemical properties of mixed WC and Pt-black powders

MAJA D. OBRADOVIĆ[1*#], BILJANA M. BABIĆ[2], ANDRZEJ KOWAL[3], VLADIMIR V. PANIĆ[1#] and SNEŽANA LJ. GOJKOVIĆ[4#]

[1]*Institute of Chemistry, Technology and Metallurgy, University of Belgrade, Njegoševa 12, 11001 Belgrade, Serbia,* [2]*Vinča Institute of Nuclear Sciences, P. O. Box 522, 11001 Belgrade, Serbia,* [3]*Institute of Catalysis and Surface Chemistry, Polish Academy of Sciences, Niezapominajek 8, 30-239 Krakow, Poland and* [4]*Faculty of Technology and Metallurgy, University of Belgrade, Karnegijeva 4, 11120 Belgrade, Serbia*

(Received 7 July, revised 28 August 2008)

Abstract: The electrochemical characteristics of a mixture of Pt-black and WC powders and its catalytic activity for methanol and formic acid oxidation were investigated in acid solution. XRD and AFM measurements revealed that the WC powder employed for the investigation was a single-phase material consisting of crystallites/spherical particles of average size of about 50 nm, which were agglomerated into much larger particles. Cyclic voltammetry showed that the WC underwent electrochemical oxidation, producing tungstate species. In the case of the mixed Pt + WC powders, the tungstate species were deposited on the Pt as a thin film of hydrous tungsten oxide. Enhanced hydrogen intercalation in the hydrous tungsten oxide was observed and it was proposed to be promoted in mixed powders by the presence of hydrogen adatoms on bare Pt sites. The determination of Pt surface area in the Pt + WC layer by stripping of underpotentially deposited Cu revealed that the entire Pt surface was accessible for underpotential deposition of Cu. Investigation of the electrochemical oxidation of methanol and formic acid on Pt + WC and pure Pt layers did not indicate electrocatalytic promotion due to the presence of WC.

Keywords: tungsten carbide; platinum; hydrogen intercalation; methanol oxidation; formic acid oxidation.

INTRODUCTION

It is expected that fuel cell research and development will provide an environmental friendly power source for vehicles and portable electronic devices. Proton exchange membrane fuel cells (PEMFC) are advantageous since they operate at low temperatures and hence do not require expensive or large containment structures. Oxygen reduction is the cathodic reaction in PEMFCs, while the oxi-

* Corresponding author. E-mail: obradovic@ihtm.bg.ac.rs
# Serbian Chemical Society member.
doi: 10.2298/JSC0812197O

dation of hydrogen or some small organic molecule occurs on the anode. Methanol distinguishes itself from other fuels because it is an inexpensive liquid and easy for handling, storage and transport.[1] Formic acid is another example since its oxidation commences at a less positive potential than methanol oxidation, while the crossover of formic acid through the polymer membrane is lower than that of methanol.[2]

Platinum is the most active single metal catalyst for the methanol oxidation reaction (MOR), although the onset potential is rather far from the thermodynamic value. Modification of Pt by various metals has been widely investigated, but there is general agreement that only Pt–Ru surfaces are much more active than single Pt. Recently, several researchers reported the use of tungsten carbide as a support for Pt particles[3,4] because of the influence of tungsten species on the activity of Pt for the MOR. Some earlier investigations of the MOR showed enhancement of the reaction rate on rare earth tungsten bronze doped with Pt,[5] platinum–tungsten oxide,[6,7] carbon-supported platinum modified with WO_y[8] and high surface area tungsten oxide containing Pt centers.[9] However, it was also reported that the presence of polyoxotungstates on Pt can suppress the interfacial formation of PtOH/PtO,[10] which participates in the oxidation process of organic molecules. On the other hand, Pt/WC exhibited a lower onset potential for CO oxidation than Pt nanoparticles supported on high surface area carbons, but the activities of Pt/WC and Pt/C for the MOR were similar.[4]

The results of an investigation of the electrochemical properties of a mixture of Pt-black and WC powders are reported in this work. The aim of the investigation was to give basic insight into the activity of the mixture in the oxidation of small organic molecules with respect to Pt alone. This study should supply additional information whether the synthesis of Pt nanoparticles supported on tungsten-based materials would be beneficial.

EXPERIMENTAL

Platinum black powder (Alfa Aesar, BET specific surface area: 24–29 $m^2 g^{-1}$) and tungsten carbide powder, provided by Woksal, Užice, Serbia, were used as the electrocatalysts. The powders were applied onto a glassy carbon substrate (Tacussel rotating disk electrode, 5 mm in diameter) from the ink to form a thin layer.[11] The Pt black powder was suspended in high purity water, while WC and the mixture of WC and Pt black were suspended in 2-propanol (Merck). In all cases, 50 μl of a Nafion® solution (5 wt. %, 1100 E.W., Aldrich) was added per 1.0 cm^3 of the suspension, in order to insure adhesion of the layer. The concentrations of Pt and WC in the suspensions were 10 and 40 mg cm^{-3}, respectively. After 1 h agitation in an ultrasonic bath (70 kHz), 5.0 μl of the suspension was placed onto a glassy carbon electrode by micro-pipette and left to dry overnight.

It should be noted that in preliminary experiments, WC and WC + Pt suspensions were prepared in water, but a certain change of the suspension and data non-reproducibility were observed. The voltammetric responses of thin layers made day by day from the same water suspension differed, indicating a decrease in the Pt surface area.

A three-compartment electrochemical glass cell with a large surface area Pt wire (99.998 % purity, Aesar) as the counter electrode and a saturated calomel electrode (SCE) as the reference electrode was used. All the potentials reported in this paper are expressed on the scale of the reversible hydrogen electrode (RHE). The supporting electrolyte of 0.10 M H_2SO_4 (Merck) was prepared with high purity water (Millipore, 18 MΩ cm resistivity). The electrolyte was deaerated by bubbling with N_2 previously purified by flowing through an ammonium metavanadate solution. Electrochemical oxidation of methanol and formic acid were investigated in deaerated supporting electrolyte which contained 0.10 M CH_3OH or 0.10 M HCOOH (Merck). The experiments were conducted at 298±0.5 K. A Pine RDE4 potentiostat and Philips PM 8143 *X–Y* recorder were employed.

WC powder was characterized by X-ray diffraction (XRD) analysis using a Siemens D500 diffractometer with CuKα radiation over the 2θ range from 10 to 90° at a scan rate of 0.04° s^{-1}. To determine the WC surface area, adsorption/desorption isotherms of N_2 were registered at –196 °C by the gravimetric McBain method. The appearance of WC powder was examined by atomic force microscopy (AFM) using a NanoScope 3D (Veeco, USA). A drop of WC suspension in 2-propanol was placed on a mica surface and left to dry. Then the imaging was performed in the contact mode using NanoProbes silicon nitride cantilevers with a force constant of 0.060 N m^{-1}.

RESULTS AND DISCUSSION

Characterization of the WC

The XRD pattern of the WC powder (Fig. 1) indicates pure single-phase WC of hcp symmetry with the lattice parameters $a_0 = b_0 = 0.29053$ nm and $c_0 = = 0.28385$ nm. The crystallite size, calculated from the width of the (101) peak using the Scherrer equation, was found to be about 40 nm. The BET real surface area of the WC was calculated to be 0.7 m^2 g^{-1}. Assuming spherical powder particles and taking 15.6 g cm^{-3} for the density of WC, a particle diameter corresponding to the BET surface area of 0.5 μm was calculated. Comparison of the XRD and BET results indicates that the particles of WC powder are compact agglomerates of smaller crystallites. This was proved by the AFM technique. The typical appearance of a WC agglomerate consisting of densely-packed, nearly spherical particles of 50 to 150 nm in size is presented in Fig. 2.

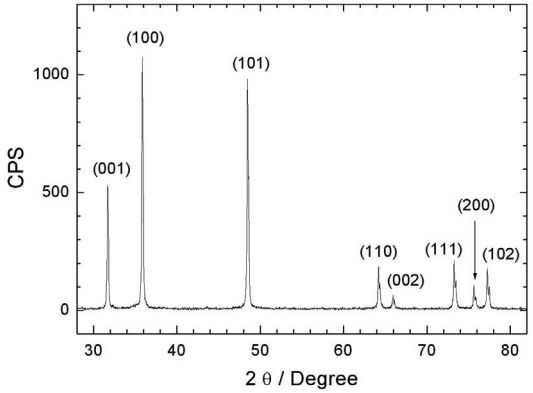

Fig. 1. XRD Pattern of the WC powder sample.

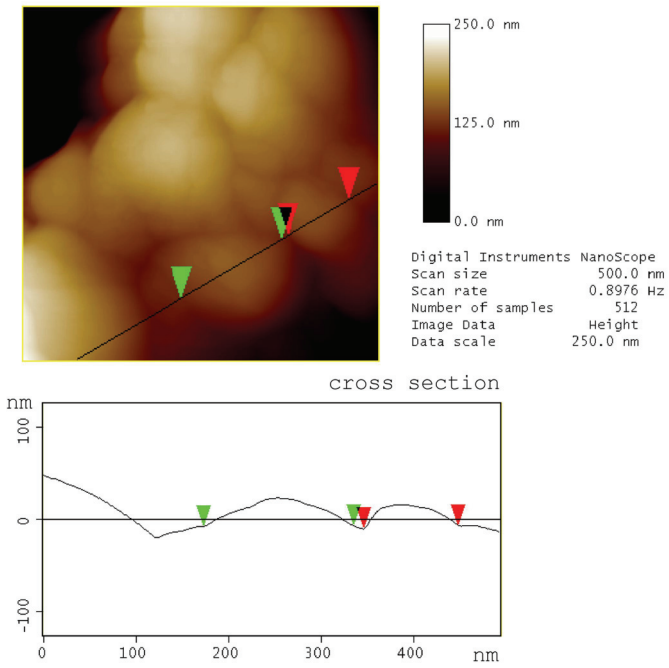

Fig. 2. The results of AFM analysis of WC powder: height image and cross section analysis.

Cyclic voltammograms of WC powder registered in 0.10 M H_2SO_4 are given in Fig. 3. When the potential was cycled between 0.050 and 0.75 V, the voltammogram was stable over time, featuring a broad anodic peak and an increase in the cathodic current at $E < 0.40$ V. In the first cycle toward more positive potentials (up to 1.25 V), an anodic peak at ≈ 1.06 V, followed by a subsequent increase in the anodic current was observed. In the second cycle, the peak and subsequent current decreased and finally reached steady-state values after the 20th cycle, as shown by the steady-state curve in Fig. 3. Upon resetting the positive potential limit back to 0.75 V, a voltammetric response like the very first one was regained.

In the presence of water and/or oxygen, WC oxidizes to surface oxide and/or soluble W(VI) species:[12,13]

$$WC + 5H_2O \rightarrow WO_3 + CO_2 + 10H^+ + 10e^- \quad (1)$$

$$WC + 6H_2O \rightarrow WO_4^{2-} + CO_2 + 12H^+ + 10e^- \quad (2)$$

The cyclic voltammogram of WC recorded in the narrow potential range (Fig. 3, 1st curve) resembles the voltammetric behavior of WO_3,[14] which indicates that the WC surface was in the oxidized state. The WO_3 layer formed spontaneously on the WC surface was partially reduced in the cathodic scan by the intercalated hydrogen:[15]

$$WO_3 + xH^+ + xe^- \rightarrow H_xWO_3 \qquad 0.1 < x < 0.5 \qquad (3)$$

The H_xWO_3 species are known as hydrogen–tungsten bronzes. The cathodic current at $E < 0.40$ V should correspond to the hydrogen intercalation process, while the broad anodic peak is very likely due to deintercalation. The anodic peak at ~1.06 V can be assigned to further oxidation of WC.[16] The products of this reaction are probably insoluble and their deposition on the electrode surface causes a decrease in the anodic current, as shown in Fig. 3.

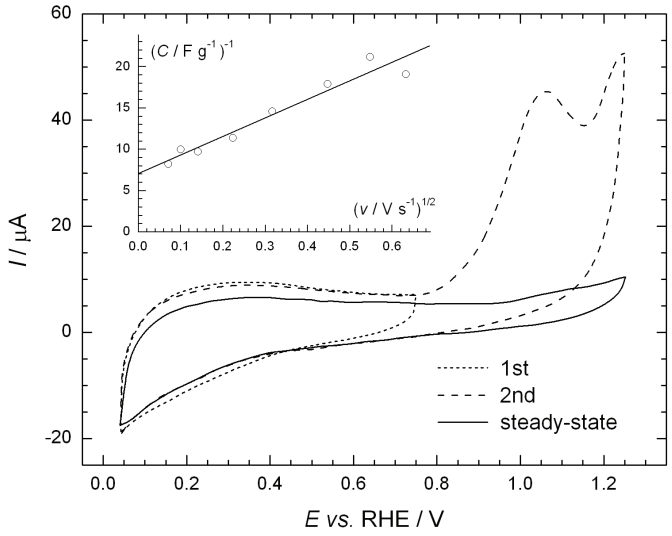

Fig. 3. The first, second and steady state cyclic voltammograms of the WC thin layer (1.27 mg WC cm^{-2}) recorded in deaerated 0.10 M H_2SO_4 at 50 mV s^{-1}. Inset: reciprocal of specific capacitance of the WC thin layer, calculated between 0.56 and 0.75 V from the steady-state voltammograms, as a function of the square root of sweep rate.

Assuming that the intercalation/deintercalation processes are accomplished at potentials above 0.55 V, the double layer capacitance of the passive film on WC was estimated from the voltammetric charge between 0.56 and 0.75 V from the steady-state voltammograms. As the inset in Fig. 3 shows, the capacitance was slightly dependent on the sweep rate, due to the porous structure. Extrapolation of the reciprocal capacitance to zero sweep rate[17] gives a total double layer capacitance of the film, C_{tot}, of 0.14 F g^{-1}. Assuming the most typical value for double layer capacitance of 20 μF cm^{-2}, a specific surface area of 0.70 m^2 g^{-1} is calculated, which coincides with the obtained BET surface area. This result indicates that native WC spherical particles within micro-sized agglomerates, as seen by AFM (Fig. 2) and calculated from XRD, are not accessible to the electrolyte, but only the surface defined by the agglomerates through the micro-pores of the layer.

Voltammetry of the Pt + WC mixture

The voltammetric behavior of mixed WC and Pt black powders is illustrated in Fig. 4. The first cycle with a positive potential limit of 0.75 V resembles the hydrogen adsorption/desorption features of Pt sites. After extension of the positive potential limit to 1.25 V, the cyclic voltammogram features the formation of Pt oxide and its reduction, as well as the development of a pair of peaks at 0.14 and 0.30 V, due to an intensive oxidation of WC. On cycling of the potential, the height of the peaks increased, while the anodic current due to the oxidation of WC decreased and eventually disappeared, similar to the behavior of pure WC powder (Fig. 3).

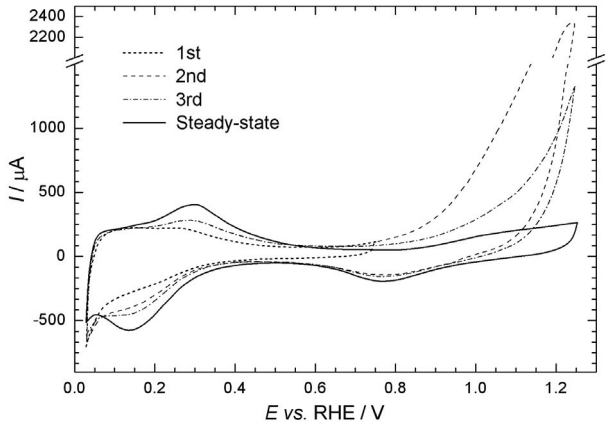

Fig. 4. Successive and steady state cyclic voltammograms of the WC + Pt thin layer (1.02 mg WC cm^{-2} + 0.25 mg Pt cm^{-2}) recorded in de-aerated 0.10 M H_2SO_4 at 50 mV s^{-1}.

The steady-state cyclic voltammograms of the single Pt black and WC powders and the mixture of Pt and WC are presented in Fig. 5. Bearing in mind that in the mixed layer and in the single layers, the amounts of Pt are identical and the amounts of WC are similar, the voltammetric charges can be directly analyzed. It is obvious from Fig. 5 that the voltammetric features of the mixture are not the simple superposition of the voltammograms of its components. The charge under the peaks at 0.14/0.30 V is significantly higher than the charge for the monolayer adsorption/desorption of hydrogen on Pt particles present in the mixture and considerably higher in comparison to the hydrogen intercalation/deintercalation charge on WC. In addition, the formation of Pt-oxide is hindered in the presence of WC. Jeon *et al.*[4] recently proposed that spillover of hydrogen from Pt to WC supplies a fresh Pt surface, resulting in the increased charge of H adsorption/desorption on the Pt sites. However, the peaks related to H adsorption/desorption on the Pt sites on the voltammogram of the Pt + WC mixture are displaced with respect to those of pure Pt or highly overlapped with the peaks at 0.14/0.30 V, related to the catalyzed oxidation of WC (Fig. 4). This observation leads to the assumption that soluble tungstate species, produced during the oxidation of WC, can be deposited onto Pt sites. The deposited layer is subjected to intercalation/deintercalation of

hydrogen, which results in the appearance of pronounced peaks at 0.14/0.30 V. When WC alone was attached to the electrode surface, anodic oxidation of WC did not produce any additional voltammetric features (Fig. 3) related to the enhanced intercalation/deintercalation process. This indicates that the deposition of intercalation-active tungstates occurs preferentially on Pt.

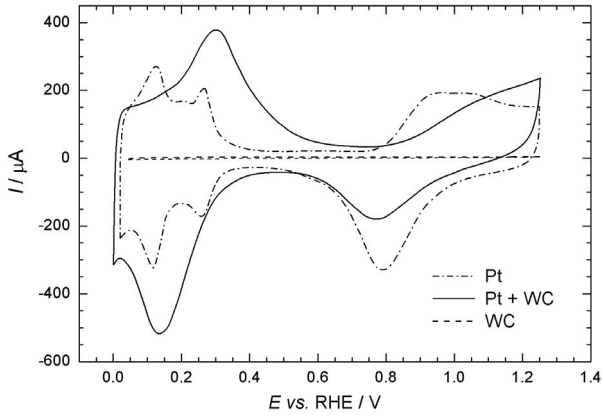

Fig. 5. Steady-state cyclic voltammograms of thin layers of WC (1.27 mg WC cm^{-2}), Pt (0.25 mg cm^{-2}) and Pt + WC (0.25 mg Pt cm^{-2} + 1.02 mg WC cm^{-2}) recorded in deaerated 0.10 M H_2SO_4 at 20 mV s^{-1}.

To calculate the pseudocapacitance of the hydrogen intercalation in the WC and WC + Pt layers, the anodic parts of the voltammograms recorded at sweep rates from 5 to 400 mV s^{-1} were integrated in the potential range from 0.050 to 0.56 V. A dependence of the pseudocapacitance on the sweep rate was registered for both the WC and WC + Pt layers. Such a behavior is due to diffusion-limited pseudocapacitive process within the porous layer of hydrous tungsten oxide formed atop the WC and Pt sites. According to the model proposed by Ardizzone *et al.*,[18] the mobility of the protons involved in Reaction (3) is hindered by the porous structure of the layer, resulting in the following pseudocapacitance *vs*. sweep rate relationships:

$$\frac{1}{C} = \frac{1}{C_{\text{tot}}} + k\sqrt{v} \tag{4}$$

$$C = C_{\text{out}} + \frac{k'}{\sqrt{v}} \tag{5}$$

where C_{tot} is the total capacitance of the porous structure, C_{out} is the capacitance of the outer layer surface (facing the bulk of the electrolyte), while the capacitance of the inner surface relates to the loose grain boundaries, C_{in}, can be calculated as $C_{\text{in}} = C_{\text{tot}} - C_{\text{out}}$.[19]

The C *vs*. $v^{-1/2}$ and C^{-1} *vs*. $v^{1/2}$ plots for WC and the mixture WC + Pt are presented in Fig. 6. Reasonably straight lines were obtained and the total pseudocapacitances were calculated. From the C *vs*. $v^{-1/2}$ plots (Fig. 6a), the pseudocapacitances related to the outer layer of hydrous tungsten oxide in both the WC

and WC + Pt layer were determined. Since the pseudocapacitances calculated in this way include the double layer capacitance, its value of 0.14 F g^{-1} (inset in Fig. 3) was subtracted. In the case of the WC + Pt mixture, the pseudocapacitance of hydrogen adsorption/desorption on Pt sites (which was found to be independent of the sweep rate) was also subtracted from the total pseudocapacitance charge. This was done assuming that hydrogen adsorption is undisturbed by the presence of WC and the products of its oxidation. The corrected pseudocapacitances of hydrogen intercalation expressed per mass of WC are given in Table I, from which it can be observed that the total pseudocapacitance is more than doubled in the presence of Pt and that the structure of the hydrous oxide layer is significantly changed. The C_{out}/C_{tot} ratio shows that for the hydrous oxide formed on WC with no Pt in the film, only about 8 % of the electroactive sites were on the surface, indicating a highly porous structure. However, when Pt was present in the film, about 80 % of the electroactive sites were easily accessible surface sites. This can be rationalized if the Pt was partially covered by thin hydrous tungsten oxide layer with the majority of its active sites being surface sites facing the electrolyte. Such a film can exhibit a higher pseudocapacitance than that on WC without Pt in the layer only if the hydrogen atoms adsorbed on Pt sites spillover to the hydrous tungsten oxide and intercalate in it.[15,20]

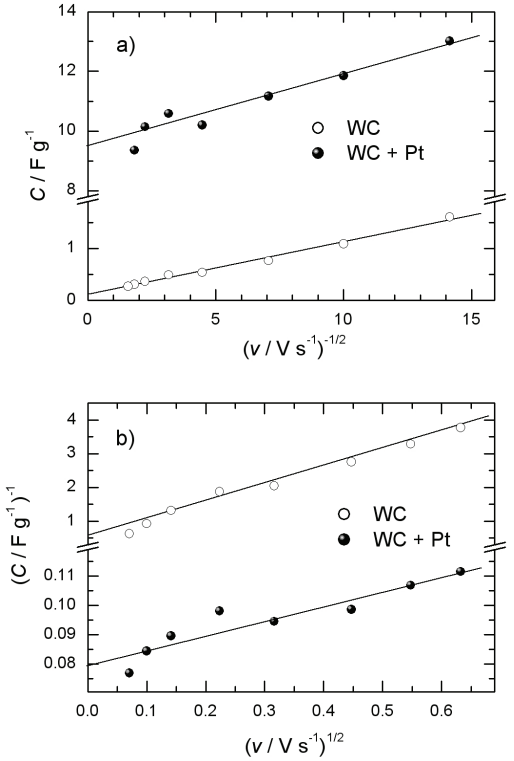

Fig. 6. a) C *vs.* $v^{-1/2}$ and b) C^{-1} *vs.* $v^{1/2}$ plots for WC and WC + Pt layer.

TABLE I. Corrected values of the pseudocapacitance for hydrogen intercalation into hydrous tungsten oxide for WC and WC + Pt thin layers, calculated per mass of WC

Electrode	C_{tot} / F g^{-1}	C_{out} / F g^{-1}	C_{out}/C_{tot}
WC	2.17	0.165	0.076
Pt + WC	4.90	3.79	0.77

Determination of the Pt surface area in the WC + Pt electrode layer

The determination of the real surface area of a catalyst is a crucial point in the assessment of its activity. The surface area of Pt can be determined from the charge of hydrogen adsorption/desorption. In the calculation, it is assumed that a complete monolayer is formed, which requires 210 μC cm^{-2}. However, the hydrogen adsorption/desorption features of Pt in the cyclic voltammogram of the WC + Pt mixture (Fig. 4) are partly discernible only when the anodic limit is set to before the onset of the oxidation of WC. After a substantial amount of WC had been oxidized, large peaks of hydrogen intercalation/deintercalation mask the Pt peaks. Therefore, some alternative method should be applied to determine Pt surface area. Recently, Green and Kucernak[21] reported that the surface area of Pt alloyed with Ru can be successfully determined from the stripping of underpotentially deposited (UPD) copper. This method is also applicable to the WC + Pt system since the anodic peak of Cu stripping is more positive than the peak for hydrogen deintercalation from the hydrous tungsten oxide. In addition, WC alone was found to be inactive for UPD Cu.

Copper was underpotentially deposited from a solution of 0.10 M H_2SO_4 and 2.0×10^{-3} M $CuSO_4$ at a potential of 0.330 V *vs*. RHE, which is about 15 mV more positive than the equilibrium potential of Cu electrodeposition in the applied electrolyte. After 2 min of deposition, which is sufficient for a complete monolayer to be formed,[21] the electrode potential was swept anodically and the stripping voltammogram was recorded. The result obtained for a polycrystalline Pt electrode and for a layer of Pt-black powder are shown in Fig. 7a and 7b, respectively. For sake of comparison, the cyclic voltammograms in the supporting electrolyte are also given. The Cu stripping curves reveal at least three different energetic states of Cu, which are similar for polycrystalline Pt and Pt-black powder. The stripping curves, corrected for the background current of Pt, were integrated and the charges were compared to the hydrogen desorption charge. The Cu(UPD)/H(UPD) ratio was calculated to be 1.8 for polycrystalline Pt and 2.3 for Pt-black, which is close to the theoretical value of 2. These results confirm that the Pt surface area can be estimated using the procedure of Cu UPD and stripping as described above. The experiment with the Pt + WC mixture show that the Cu stripping peak is shifted anodically but the charge beneath the peak corresponds to the surface area of Pt in the layer.

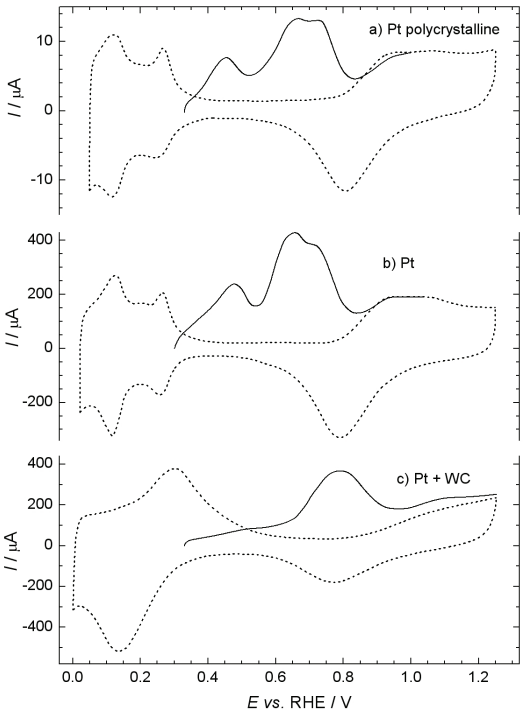

Fig. 7. Cyclic voltammograms of: a) Pt polycrystalline electrode, b) thin layer of Pt (0.25 mg cm^{-2}) and c) thin layer of Pt + WC (0.25 mg Pt cm^{-2} + 1.02 mg WC cm^{-2}) recorded in 0.10 M H_2SO_4 (dashed lines) and Cu stripping voltammograms recorded in the presence of 2.0×10^{-3} M $CuSO_4$ (solid lines) at 20 mV s^{-1}.

Voltammetric experiments for the Pt + WC mixture revealed that a thin layer of hydrous tungsten oxide was deposited on Pt (Figs. 4 and 5, Table I). However, Cu stripping showed that the entire surface area of Pt in the film was accessible to Cu UPD. It should also be noted that formation of Pt-oxide was hindered by the presence of WC (Fig. 4) and that the Cu stripping peak was shifted anodically with respect to the peak on pure Pt (Fig. 7). Thus, it can be anticipated that small organic molecules, such as CH_3OH and HCOOH, would be able to approach the Pt surface through the tungsten oxide film, but the electrocatalytic properties of the Pt might be changed due to the presence of the film, as indicated in the literature.[5–9]

Oxidation of methanol and formic acid

The oxidation of methanol and formic acid were investigated on a layer of the WC + Pt mixture after the steady-state voltammogram (Fig. 5) had been established. Methanol or formic acid was added into the cell while holding the potential at 0.10 V. After 2 min, a potential sweep was applied at a rate of 1.0 mV s^{-1} and the polarization curve was recorded. Concerning the results of Cu stripping on the WC + Pt mixture, the current densities were calculated with respect to the entire surface area of Pt in the catalyst layer, assuming that the Pt sites were equally available for UPD of Cu and the oxidation of the organics. The same

experiments were performed on pure Pt-black layers and the results were compared. The diagrams in Fig. 8 show overlapping of the results for pure Pt and the WC + Pt mixture, meaning that hydrous tungsten oxide formed by the oxidation of WC does not influence the activity of Pt for the oxidation of methanol and formic acid.

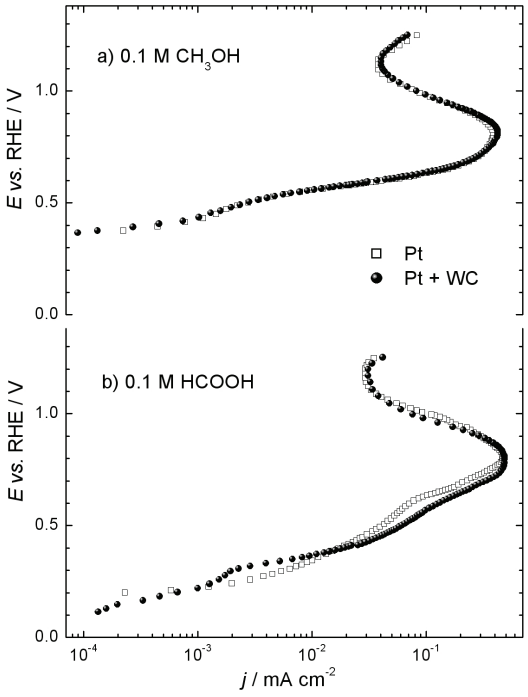

Fig. 8. Tafel plots for the oxidation of a) 0.10 M CH_3OH and b) 0.10 M HCOOH on the thin layers of Pt and WC + Pt in deaerated 0.10 M H_2SO_4. Sweep rate: 1.0 mV s^{-1}.

CONCLUSIONS

Cyclic voltammetry revealed that WC undergoes electrochemical oxidation, which produces tungstate species. In the case of the mixed WC + Pt powders, these species appeared to be deposited onto Pt in a form of a hydrous tungsten oxide. Enhanced hydrogen intercalation in the hydrous tungsten oxide was observed and it is proposed that this process was promoted by the spillover of the hydrogen adatoms on the bare Pt sites. The presence of WC in the Pt catalyst layer had no effect on the kinetics of methanol and formic acid oxidation, assuming that the part of Pt surface covered by hydrous tungsten oxide did not hinder the approach of the organics to the Pt beneath.

Acknowledgements. This work was financially supported by the Ministry of Science of the Republic of Serbia, contract Nos. 142048 and 142056.

ИЗВОД

ЕЛЕКТРОХЕМИЈСКА СВОЈСТВА СМЕШЕ ПРАХОВА WC И Pt

МАЈА Д. ОБРАДОВИЋ[1], БИЉАНА М. БАБИЋ[2], ANDRZEJ KOWAL[3], ВЛАДИМИР В. ПАНИЋ[1] и СНЕЖАНА Љ. ГОЈКОВИЋ[4]

[1]Институт за хемију, технологију и металургију, Универзитет у Београду, Његошева 12, 11001 Београд, [2]Институт за нуклеарне науке "Винча", п. пр. 522, 11001 Београд, [3]Institute of Catalysis and Surface Chemistry, Polish Academy of Sciences, Niezapominajek 8, 30-239 Krakow, Poland и [4]Технолошко–металуршки факултет, Универзитет у Београду, Карнегијева 4, 11120 Београд

У раду су испитиване електрохемијске карактеристике смеше прахова Pt и WC и њена каталитичка активност за реакције оксидације метанола и мрављe киселине у киселом раствору. Анализа резултата дифракције X-зрака (XRD) и микроскопије атомских сила (AFM) показују да је прах WC једнофазни материјал са просечном величином кристалита од око 50 nm, који су агломерисани у много веће честице. Циклична волтаметрија указује на то да WC подлеже оксидацији којом настају волфраматне врсте. У случају смеше прахова Pt и WC, волфраматне врсте највероватније се таложе на Pt у облику танког слоја хидратисаних оксида волфрама. Примећено је повећање интеркалације водоника у слоју хидратисаних волфрамата и претпоставља се да присуство адатома водоника на површини Pt потпомаже процес водоничне интеркалације. Одређивање површине Pt у слоју Pt + WC десорпцијом монослоја Cu таложеног на потпотенцијалима указује да је читава површина Pt доступна за таложење атома Cu. Испитивање електрохемијских реакција оксидације метанола и мрављe киселине на слоју смеше Pt + WC и слоју чисте Pt указује да присуство праха WC не утиче на електрокаталитичка својства Pt.

(Примљено 7. јула, ревидирано 28. августа 2008)

REFERENCES

1. S. Wasmus, A. Küver, *J. Electroanal. Chem*. **461** (1999) 14
2. X. Yu, P. Pickup, *J. Power Sources* **182** (2008) 24
3. R. Ganesan, J. S. Lee, *Angew. Chem. Int. Ed*. **44** (2005) 6557
4. M. K. Jeon, H. Daimon, K. R. Lee, A. Nakahara, S. I. Woo, *Electrochem. Commun*. **9** (2007) 2692
5. K. Machida, M. Enyo, G. Adachi, J. Shiokawa, *J. Electrochem. Soc*. **135** (1988) 1955
6. M. B. Oliveira, L. P. R. Profeti, P. Olivi, *Electrochem. Commun*. **7** (2005) 703
7. P. K. Shen, A. C. C. Tseung, *J. Electrochem. Soc*. **141** (1994) 3082
8. A. K. Shukla, M. K. Ravikumar, A. S. Aricò, G. Candiano, V. Antonucci, N. Giordano, A. Hamnett, *J. Appl. Electrochem*. **25** (1995) 528
9. C. Bock, B. MacDougall, *Electrochim. Acta* **47** (2002) 3361
10. M. Chojak, A. Kolary-Zurowska, R. Wlodarczyk, K. Miecznikowski, K. Karnicka, B. Palys, R. Marassi, P. Kulesza, *Electrochim. Acta* **52** (2007) 5574
11. S. Lj. Gojković, A. V. Tripković, R. M. Stevanović, *J. Serb. Chem. Soc*. **72** (2007) 1419
12. J. D. Voorhies, *J. Electrochem. Soc*. **119** (1972) 219
13. M. H. Ghandehari, *J. Electrochem. Soc*. **127** (1980) 2144
14. E. J. McLeod, V. I. Birss, *Electrochim. Acta* **51** (2005) 684
15. P. J. Kulesza, L. R. Faulkner, *J. Electrochem. Soc*. **136** (1989) 707
16. H. Chhina, S. Campbell, O. Kesler, *J. Power Sources* **164** (2007) 431

17. R. De Levie, in *Advances in electrochemistry and electrochemical engineering*, Vol. 6, P. Delahay Ed., Interscience, New York, 1967, p. 329
18. S. Ardizzone, G. Fregonara, S. Trasatti, *Electrochim. Acta* **35** (1990) 263
19. V. Panić, A. Dekanski, S. Milonjić, V. B. Mišković-Stanković, B. Nikolić, *J. Serb. Chem. Soc.* **71** (2006) 1173
20. J. Shim, C.-R. Lee, H.-K. Lee, J.-S. Lee, E. J. Cairns, *J. Power Sources* **102** (2001) 172
21. C. L. Green, A. Kucernak, *J. Phys. Chem. B* **106** (2002) 1036.